

Blast-wave analysis of strange particle m_T spectra in Pb-Pb collisions at the SPS

G E Bruno for the NA57 Collaboration †

Dipartimento IA di Fisica dell'Università e del Politecnico di Bari and INFN, Bari, Italy

Abstract. The transverse mass spectra of high statistics, high purity samples of K_S^0 , Λ , Ξ and Ω particles produced in Pb-Pb collisions at SPS energy have been studied in the framework of the blast-wave model. The dependence of the freeze-out parameters on particle species and event centrality is discussed. Results at 40 A GeV/c are presented here for the first time.

PACS numbers: 12.38.Mh, 25.75.Nq, 25.75.Ld, 25.75.Dw

1. Introduction

The experimental programme with heavy-ion beams at CERN SPS is aimed at the study of the behaviour of hadronic matter under extreme conditions of temperature, pressure and energy density. Within this programme, NA57 is a dedicated experiment for the study of the production of strange and multi-strange particles in Pb-Pb and p-Be collisions at mid-rapidity [1]. Results on strange particle yields, ratios and strangeness enhancements with respect to p-Be reactions are discussed in a separate contribution to this conference [2].

In this paper we present a study of the transverse mass ($m_T = \sqrt{p_T^2 + m^2}$) spectra for Λ , Ξ^- , Ω^- hyperons, their antiparticles and K_S^0 measured in Pb-Pb collisions at 158 and 40 A GeV/c. The shapes of the m_T spectra are expected to be determined both by the thermal motion of the particles and by a pressure-driven collective flow. To disentangle the two contributions we rely on the *blast-wave* model [3, 4], which assumes cylindrical symmetry for an expanding fireball in local thermal equilibrium, testing different hypotheses on the transverse flow profile.

2. Data sample and analysis

The results presented in this paper are based on the analysis of the full data sample collected in Pb-Pb collisions, consisting of 460 M events at 158 A GeV/c and 240 M events at 40 A GeV/c. The selected sample of events corresponds to the most central 53% of the inelastic Pb-Pb cross-section. The data sample has been divided into five centrality classes (0,1,2,3 and 4, class 4 being the most central) according to the

† For the full author list see Appendix “Collaborations” in this volume.

value of the charged particle multiplicity around central rapidity measured by a Silicon Microstrip Multiplicity Detector. The procedure for the measurement of the multiplicity distribution and the determination of the collision centrality for each class is described in reference [5]. The fractions of the inelastic cross-section for the five classes, calculated assuming a total cross-section of 7.26 barn, are given in table 1.

Table 1. Centrality ranges for the five classes.

Class	0	1	2	3	4
σ/σ_{inel} (%)	40 to 53	23 to 40	11 to 23	4.5 to 11	0 to 4.5

The experimental procedure for the determination of the m_T distribution is described in reference [6], where the results at 158 A GeV/c are discussed in detail.

3. Exponential fits of the transverse mass spectra at 158 A GeV/c

The inverse slope parameter T_{app} (“apparent temperature”) has been extracted by means of a maximum likelihood fit of the measured distribution of the invariant differential cross-section $\frac{d^2N}{m_T dm_T dy}$ to the formula $f(y) \exp\left(-\frac{m_T}{T_{app}}\right)^\ddagger$. The apparent temperature is interpreted as due to the thermal motion coupled with a collective transverse flow of the fireball components [3, 4]. The $1/m_T dN/dm_T$ distributions are shown in figure 1 for the five centrality classes and the inverse slope parameters T_{app} are given in table 2.

An increase of T_{app} with centrality is observed in Pb-Pb for Λ , Ξ^- and possibly

Table 2. Inverse slopes (MeV) of the m_T distributions for the five Pb-Pb centrality classes (0,4), and for p-Be and p-Pb interactions [7] at 158 A GeV/c. Only statistical errors are shown. In Pb-Pb, systematic errors are estimated to be 10% for all centralities.

	p-Be	p-Pb	0	1	2	3	4
K_S^0	197 ± 4	217 ± 6	239 ± 15	239 ± 8	233 ± 7	244 ± 8	234 ± 9
Λ	180 ± 2	196 ± 6	237 ± 19	274 ± 13	282 ± 12	315 ± 14	305 ± 15
$\bar{\Lambda}$	157 ± 2	183 ± 11	277 ± 19	264 ± 11	283 ± 10	313 ± 14	295 ± 14
Ξ^-	202 ± 13	235 ± 14	290 ± 20	290 ± 11	295 ± 9	304 ± 11	299 ± 12
Ξ^+	182 ± 17	224 ± 21	232 ± 29	311 ± 23	294 ± 18	346 ± 28	356 ± 31
$\Omega^- + \bar{\Omega}^+$	169 ± 40	334 ± 99	274 ± 34		274 ± 28	268 ± 23	

also for $\bar{\Lambda}$. Inverse slopes for p-Be and p-Pb collisions [7] are also given in table 2. In central and semi-central Pb-Pb collisions (i.e. classes 1 to 4) we observe baryon-antibaryon symmetry in the shapes of the spectra. Such a symmetry is not present in p-Be collisions. The similarity of baryon and antibaryon m_T slopes observed in Pb-Pb suggests that strange baryons and antibaryons may be produced by similar mechanisms.

\ddagger The rapidity distribution is assumed to be flat within our acceptance region corresponding to about half a unit of rapidity around mid-rapidity.

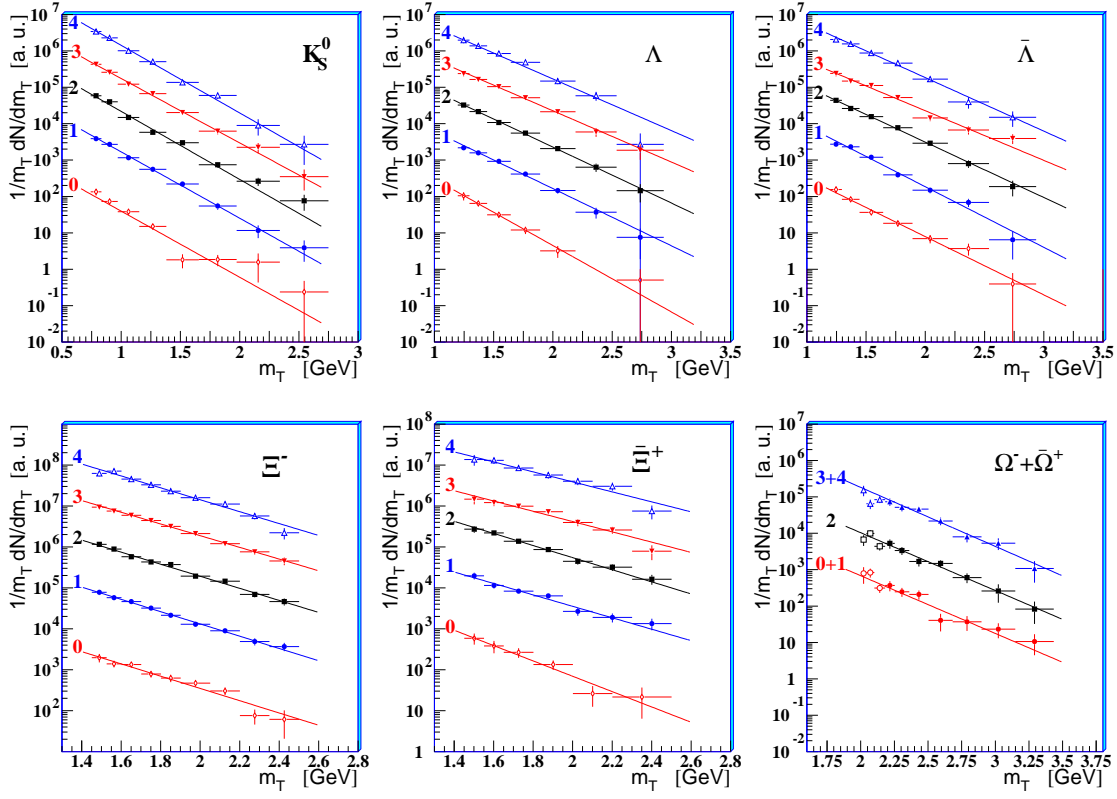


Figure 1. Transverse mass spectra of the strange particles in Pb-Pb collisions at 158 A GeV/c for the five centrality classes of table 1. For each species, class 4 is displayed uppermost and class 0 lowermost.

4. Blast-wave description of the spectra in Pb-Pb collisions

The blast-wave model [3] predicts a double differential cross-section for particle j of the form:

$$\frac{d^2 N_j}{m_T dm_T dy} = \mathcal{A}_j \int_0^{R_G} m_T K_1 \left(\frac{m_T \cosh \rho}{T} \right) I_0 \left(\frac{p_T \sinh \rho}{T} \right) r dr \quad (1)$$

where $\rho(r) = \tanh^{-1} \beta_{\perp}(r)$ is a transverse boost, K_1 and I_0 are modified Bessel functions, R_G is the transverse geometric radius of the source at freeze-out and \mathcal{A}_j is a normalization constant. The transverse velocity field $\beta_{\perp}(r)$ has been parametrized according to a power law:

$$\beta_{\perp}(r) = \beta_S \left[\frac{r}{R_G} \right]^n \quad r \leq R_G \quad (2)$$

With this type of profile the numerical value of R_G does not influence the shape of the spectra but just the absolute normalization (i.e. the constant \mathcal{A}_j). The parameters which can be extracted from a fit of equation 1 to the experimental spectra are thus the thermal freeze-out temperature T and the *surface* transverse flow velocity β_S . Assuming a uniform particle density, the latter can be connected to the *average* transverse flow velocity using the expression $\langle \beta_{\perp} \rangle = \frac{2}{2+n} \beta_S$.

4.1. Global fit with different profiles

The results of the fits with different profile hypotheses (i.e. different values of the exponent n) are given in table 3. The values of T and $\langle \beta_{\perp} \rangle$ are found to be statistically

Table 3. Results of the blast-wave model fit using different transverse flow profiles. The quoted errors are statistical. The systematic errors on the temperature and on the velocities are estimated to be about 10% and 3%, respectively, for all the four profiles.

	$n = 0$	$n = 1/2$	$n = 1$	$n = 2$
158 A GeV/c				
T (MeV)	158 ± 6	152 ± 6	144 ± 7	151 ± 11
$\langle \beta_{\perp} \rangle$	0.396 ± 0.015	0.394 ± 0.013	0.381 ± 0.013	0.316 ± 0.014
χ^2/ndf	39.6/48	36.9/48	37.2/48	68.0/48
40 A GeV/c				
T (MeV)	128 ± 4	123 ± 3	118 ± 5	123 ± 7
$\langle \beta_{\perp} \rangle$	0.432 ± 0.012	0.423 ± 0.008	0.398 ± 0.010	0.325 ± 0.011
χ^2/ndf	62/34	65/34	79/34	150/34

anti-correlated; the systematic errors on T and $\langle \beta_{\perp} \rangle$, instead, are correlated: they are estimated to be 10% and 3%, respectively, at both energies. The use of the three profiles $n=0, 1/2$ and 1 results in similar values of the freeze-out temperatures and of the average transverse flow velocities. Profiles with $n \geq 2$ are disfavoured by the data.

In the following, a linear ($n = 1$) r -dependence of the transverse flow velocity is used. The global fits of equation 1 to the data points of all the measured strange particle spectra and the corresponding 1σ contour plots are shown in figure 2. A lower thermal freeze-out temperature is measured at lower beam energy but the transverse flow

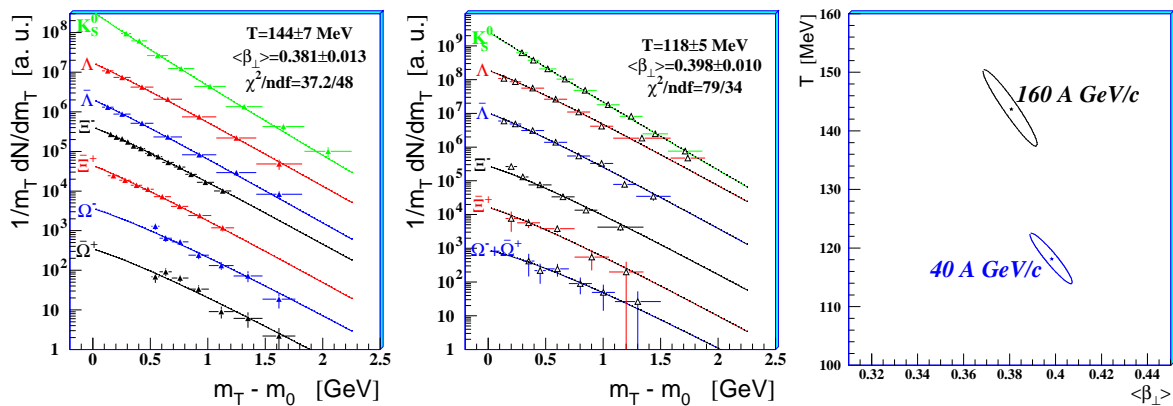


Figure 2. Blast-wave fits to the transverse mass spectra of strange particles for the 53% most central Pb-Pb cross-section at 158 (left) and at 40 (middle) A GeV/c.

Right: contour plots in the $\langle \beta_{\perp} \rangle - T$ plane at the 1σ confidence level.

velocities are found to be compatible in the errors. At 40 A GeV/c, a large contribution to the χ^2 comes from the Ξ spectra: the possibility of an early freeze-out of multi-strange particles is discussed below.

4.2. Particles with/without quarks in common with the nucleon.

The particles have been divided into two groups — those which share valence quarks with the nucleons and those which do not — since it is known that the particles of the two groups may exhibit different production features. Results of separate blast-wave fits are given in table 4. The freeze-out conditions are compatible within two sigmas. Since

Table 4. Thermal freeze-out temperature and average transverse flow velocity in the full centrality range. The first error is statistical, the second one systematic.

particles	\mathbf{T} (MeV)	$\langle \beta_{\perp} \rangle$	χ^2/ndf
158 A GeV/c			
K_S^0, Λ, Ξ^-	$146 \pm 8 \pm 14$	$0.376 \pm 0.015 \pm 0.012$	18.1/23
$\bar{\Lambda}, \bar{\Xi}^+, \Omega^-, \bar{\Omega}^+$	$130 \pm 28 \pm 14$	$0.403 \pm 0.032 \pm 0.012$	18.5/23
40 A GeV/c			
K_S^0, Λ, Ξ^-	$119 \pm 5 \pm 11$	$0.40 \pm 0.01 \pm 0.01$	56.6/18
$\bar{\Lambda}, \bar{\Xi}^+, \Omega^-, \bar{\Omega}^+$	$80 \pm 19 \pm 11$	$0.45 \pm 0.03 \pm 0.01$	14.8/18

the interaction cross-sections for the particles of the two groups are quite different, this finding would suggest limited importance of final state interactions (i.e. a rapid thermal freeze-out) and similar production mechanisms for the two groups.

4.3. Earlier freeze-out of multi-strange particles ?

The 1σ contours of the separate blast-wave fits for singly and multiply strange particles are shown in figure 3.

At 158 A GeV/c, the results of the fits for both groups of particles are compatible with the result of the global fit determination. However, the fit for the multiply strange particles is statistically dominated by the Ξ ; in fact the $\Xi+\Omega$ contour remains essentially unchanged when fitting the Ξ alone. For the Ω , due to the lower statistics, it is not possible to extract significant values for both freeze-out parameters from its spectrum alone (as can be done for the Ξ). Any possible deviation for the Ω from the freeze-out systematics extracted from the combined fit to the K_S^0 , Λ and Ξ spectra can only be inferred from the integrated information of the Ω spectrum, i.e. from its inverse slope. In figure 3 we plot a compilation of inverse slopes measured in Pb-Pb collisions, superimposed to blast-wave model results. The full lines represent the inverse slope one would obtain by fitting an exponential to a “blast-like” $1/m_T dN/dm_T$ distribution for a generic particle of mass m_0 , in the common range $0.05 < m_T - m_0 < 1.50$ GeV/c², for two different freeze-out conditions: absence of transverse flow ($\langle \beta_{\perp} \rangle = 0$) and our best

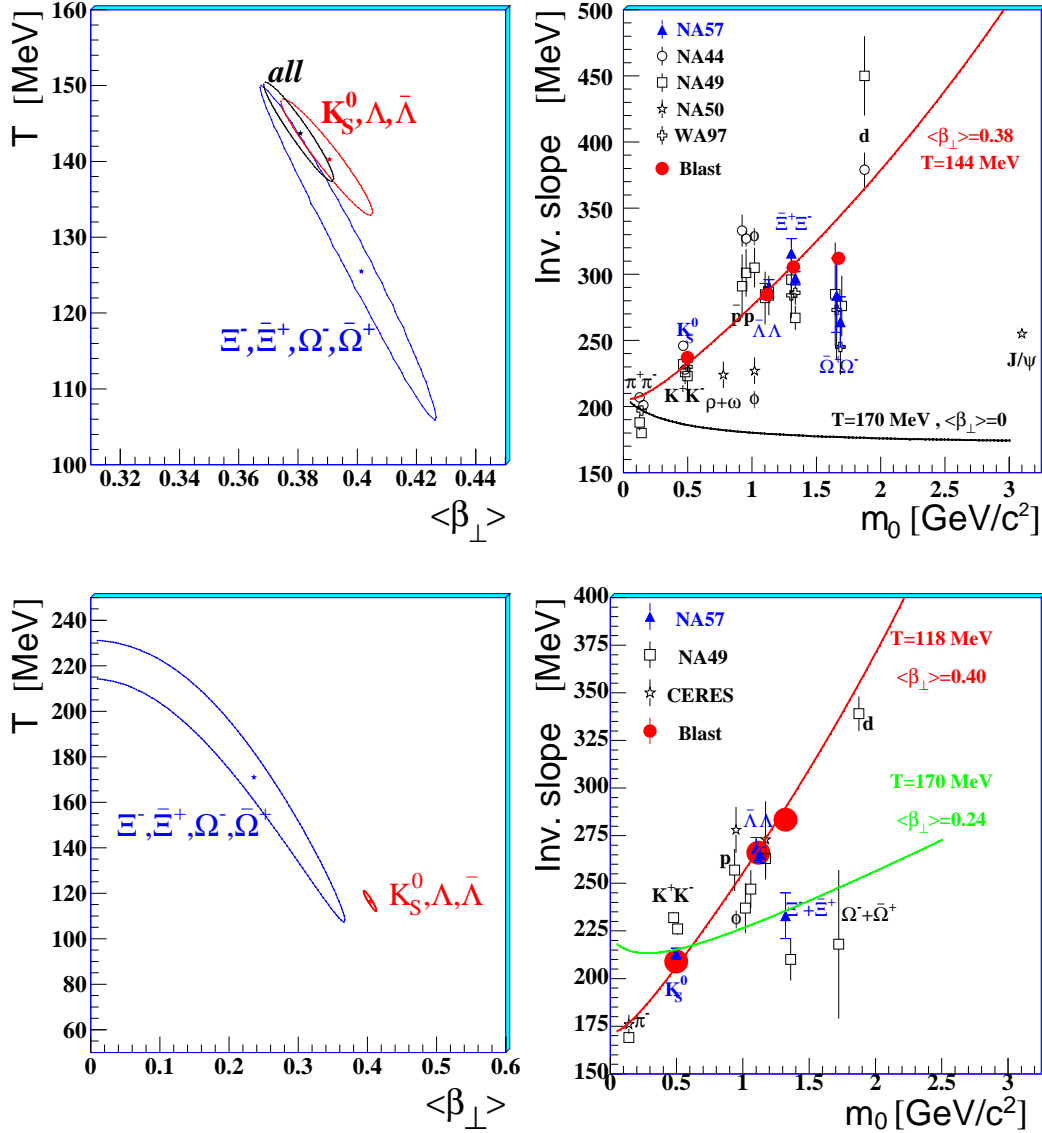


Figure 3. Top: 158 A GeV/c, bottom: 40 A GeV/c.

Left: the thermal freeze-out temperature versus the average transverse flow velocity for blast-wave fits using a linear ($n = 1$) velocity profile. The 1σ contours are shown, with the markers indicating the optimal fit locations. Right: prediction of the blast-wave model for inverse slopes (see text for details).

fit determination. Since the inverse slope is a function of the $m_T - m_0$ range where the fit is performed, we have also computed the blast-wave inverse slopes of K_S^0 , Λ , Ξ and Ω spectra in the $m_T - m_0$ ranges of NA57 (closed circles). The measured values of the inverse slope of the Ω appear to deviate from the trend of the other strange particles.

At 40 A GeV/c the same analysis suggests an early decoupling even of the Ξ with respect to the singly strange particles (see figure 3).

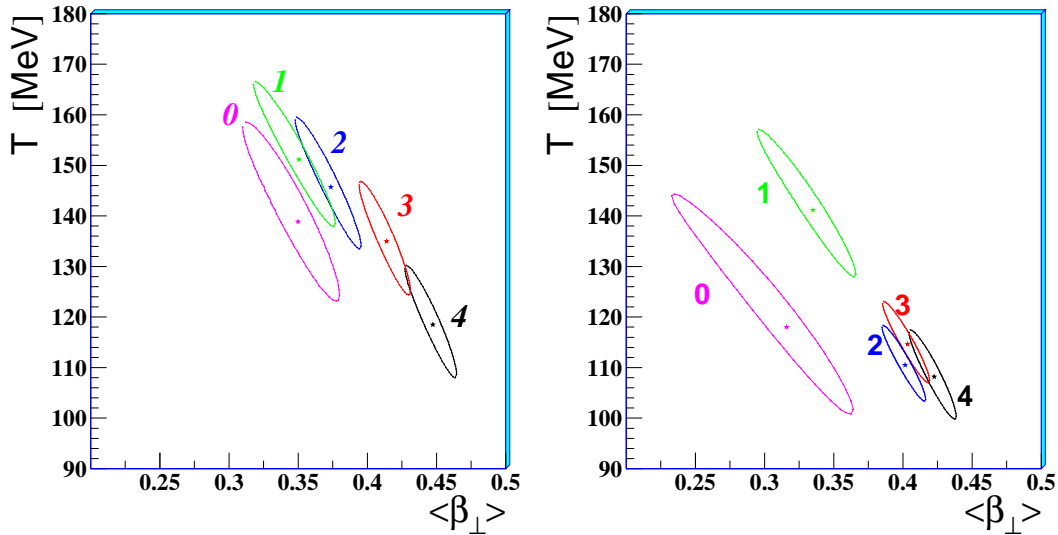


Figure 4. The 1σ confidence level contours at 158 (left) and 40 (right) A GeV/ c .

4.4. Centrality dependence

In figure 4 we show the 1σ confidence level contours for each of the five centrality classes defined in table 1. The observed trend is as follows: the more central the collisions the larger the transverse collective flow and the lower the final thermal freeze-out temperature. Higher freeze-out temperatures for more peripheral collisions may be interpreted as the result of an earlier decoupling of the expanding system. Therefore, when trying to describe hydro-dynamically the experimental data measured for peripheral or semi-central collisions, one should employ higher values of the freeze-out temperature than the 120 MeV measured for central collisions. Indeed, in reference [10] the measured elliptic flow for Pb-Pb at 158 A GeV/ c in the centrality range $\sigma/\sigma_{geo} = (13 - 26)\%$ is close to that obtained with a hydro-dynamical evolution terminated at $T = 160$ MeV. In the range $\sigma/\sigma_{geo} = (11 - 23)\%$ we measure $T = 146 \pm 17$ MeV.

5. Conclusions

The analysis of the transverse mass spectra of strange particles in Pb-Pb collisions at SPS energies suggests that after a central collision the system expands explosively and then it freezes-out when the temperature is of the order of 120 MeV, with an average transverse flow velocity of about one half of the speed of light. Similar transverse flow velocities are measured at 40 and 158 A GeV/ c but the freeze-out temperature is lower at the lower energy. The inverse slopes of multi-strange particles (Ω at 158 A GeV/ c , Ξ and Ω at 40 A GeV/ c) appear to deviate from the values predicted by the blast-wave model tuned on singly-strange particles (K_S^0 , Λ and $\bar{\Lambda}$). Finally, the results on the centrality dependence of the expansion dynamics indicate that with increasing centrality the transverse flow velocity increases and the freeze-out temperature decreases.

References

- [1] Caliandro R *et al.*, NA57 proposal, 1996 *CERN/SPSLC 96-40*, *SPSLC/P300*
- [2] Elia D *et al.*, contribution to these proceedings
- [3] Schnedermann E, Sollfrank J and Heinz U 1993 *Phys. Rev. C* **48** 2462
- [4] Schnedermann E, Sollfrank J and Heinz U 1994 *Phys. Rev. C* **50** 1675
- [5] Carrer N *et al.* 2001 *J. Phys. G: Nucl. Phys.* **27** 391
- [6] Antinori F *et al.* 2004 *J. Phys. G: Nucl. Phys.* **30** 823-840
Bruno G E *et al.* 2004 *J. Phys. G: Nucl. Phys.* **30** S717-S724
- [7] Fini R A *et al.* 2001 *Nucl. Phys. A* **681** 141c
- [8] van Hecke H, Sorge H and Xu N 1998 *Phys. Rev. Lett.* **81** 5764
- [9] Antinori F *et al.* 2000 *Eur. Phys. J. C* **14** 633
- [10] Agakichiev G. *et al.* 2004 *Phys. Rev. Lett.* **92** 032301